Design of High Strength Steel Longitudinal Stiffened Plate Girders Loaded with combined Bending, Shear and Compression

Filipa Alexandra Clemente Ribeiro Baguinho

Abstract

This paper presents the numerical analysis of S690 high-strength steel plate girders, with welded sections, loaded under combined bending, shear and compression. The ultimate strength of steel plate girders is evaluated using formulations according to the recent prEN 1993-1-5 regarding both methods proposed in the standard, the Effective Width Method (EWM) and the Reduced Stress Method (RSM). Additionally, a new method considering the possibility of stress shedding from the web to the flanges on the RSM is introduced (RSM+S). A parametric study is carried out to compare the results given by these methods and results obtained by the GMNIA numerical analysis of plate girders with one longitudinal closed stiffener placed at several different positions along the compressed part of the web.

Keywords: N-M-V interaction, EN 1993-1-5, high strength steel S690, slender plate girder, longitudinal stiffeners, cable stayed bridges.

1. Overview

Slender plate girders strengthened with transverse and longitudinal stiffeners have been increasingly used in the design of cable-stayed bridges with medium to long spans in the past few years. However, the design of cable-stayed bridge decks supported by the slender plate I-girders is a challenging mission as they are subjected to high compression forces transmitted by the stays, along with the bending and shear produced by the vertical loads. Thus, to ensure the safety of these steel I-girders, the design should consider the combined N-M-V interaction. This interaction can follow the formulations present in the current version of EN1993-1-5 [1]. However, it is known that this formulation does not give the best assessment of the real interaction of the forces. In that regard, it is worth noting the investigations conducted by Sinur and Beg [2,3], and Jáger and Kövesdi [4,5,6], that have numerically and experimentally investigated the bending-shear interaction (M-V interaction) without compression for a large range of stiffened and unstiffened I-girders. Based on these studies some enhancements have been introduced in the prEN1993-1-5 [7], namely in the bending-shear interaction formulas.

Recently, Biscaya studied the behaviour of S355 steel plate girders submitted to the combined N-M-V forces [8], and proposed some improvements in the design N-M-V interaction formulation [9]. This formulation has been tested for high strength steel S690 plate girders with only transverse stiffeners [10] and proved to give good results as well. Thus, the main goal of this study is to extend the application of the proposed formulation for the case of for high strength steel S690 longitudinally stiffened slender plate girders and investigate the optimum position of the longitudinal closed stiffener when the girder is loaded under pure bending, shear and compression, and also when all three N-M-V internal forces are present, as is the case of plate girders of steel and composite stayed-cable decks.

According to the prEN 1993-1-5 [7] when using the effective width method (EWM), the design check of N-M-V interaction of slender steel plate girders (Fig. 1) is made according to references [7,9]. The N-M-V interaction surface has a discontinuity at 45º in the N-M plane (Fig. 2), depending on whether the web is fully compressed, which is not in accordance with the predicted continuous resistance behaviour.

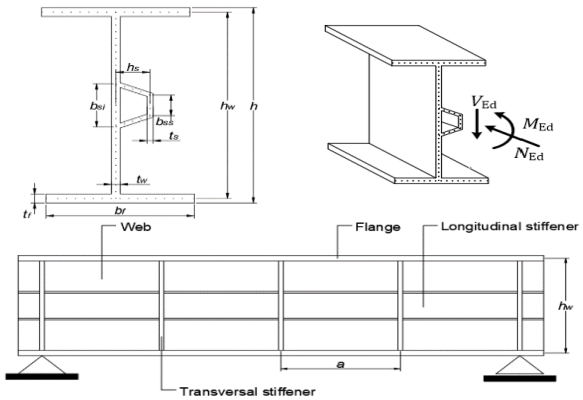

Fig. 1: Design of S690 slender plate I-girders under combined bending, shear and compression [10]

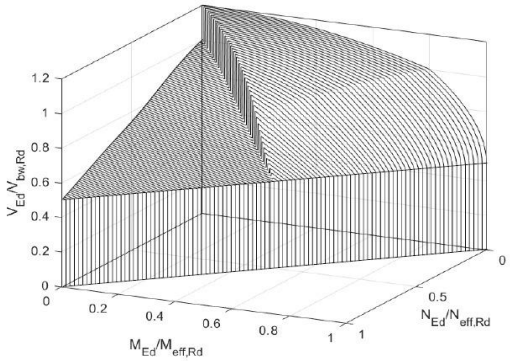

Fig. 2: N-M-V interaction diagram given by prEN1993-1-5 [7]

2. Plate girder geometries and the critical stresses

2.1 Investigated plate girder geometries

To investigate structural behaviour and identify the optimal position of the longitudinal stiffener, five plate girder designs are chosen. The investigated plate girder geometries have the following parameters: $h_w/t_w = 80$; $h_w = 1000$ mm; $b_{si} = 100$ mm; $b_{ss} = 50$ mm; $\gamma = 50$; $\alpha = 1$; $A_f/A_w = [0\,;1.0]$, and one closed longitudinal stiffener located at $[0.50\,h_w; 0.60\,h_w; 0.67\,h_w; 0.75\,h_w; 0.80\,h_w]$; without stiffener, it is assumed to be placed at h_w level.

2.2 Calculation of the critical stresses

The critical stresses for the design of stiffened plates are based on the prEN 1993-1-5 - Annex A formulation [7]. For this design of the stiffened plate, an interaction between the plate-like and column-like behaviours is assumed.

Local plate-buckling critical stress

$$\sigma_{cr.loc} = k_\sigma \times \frac{\pi^2 E}{12(1-\nu^2)} \times \left(\frac{t_w}{b_i}\right)^2 \quad (1)$$

Elastic critical column buckling stress

$$\sigma_{cr.sl} = \frac{\pi^2\, E\, I_{sl.1}}{A_{sl.1}\, a^2} \quad (2)$$

Global plate-buckling of the stiffened plate critical stress

$$\sigma_{cr.p} = \sigma_{cr.sl} = \frac{1{,}05\, E}{A_{sl.1}} \times \frac{\sqrt{I_{sl.1}\, {t_w}^3 h_w}}{b_I\, b_{II}} \quad \text{for } a \geq a_c$$

$$\sigma_{cr.p} = \sigma_{cr.sl} = \frac{\pi^2\, E\, I_{sl.1}}{A_{sl.1}\, a^2} + \frac{E\, t_w^3\, h_w\, a^2}{4\pi^2\,(1-\nu^2)\, A_{sl.1}\, b_I^2\, b_{II}^2} \quad \text{for } a \geq a_c \quad (3)$$

$$a_c = 4{,}33 \times \sqrt[4]{\frac{I_{sl.1}\, b_I^2\, b_{II}^2}{t_w^3\, h_w}} \quad (4)$$

3. Numerical model for non-linear analysis

3.1 Model assumptions

Several numerical models were built up using the multi-purpose code Abaqus-Python [11] interpreter and Matlab subroutines. The analysis is conducted using the Modified Riks Method [11] and include equivalent geometric imperfections and material non-linearity (GMNIA). Modified Riks Method is chosen as it allows the convergence problems associated with solving non-linear systems of equations to be overcome, by using an iterative procedure of variation of the applied load. Several models were studied to find out which model allows to reproduce the structural behaviour with enough accuracy. It was concluded that considering a square panel ($\alpha = 1$), 30 quadrangular elements along the longitudinal edges attend the purpose of this investigation. For the boundary conditions, studies were carried out to understand which ones better suited this study, confirming that the longitudinally stiffened plate-girders and I-girders should be designed with the four edges simply supported. A 3-panel model of Figure 3 is used.

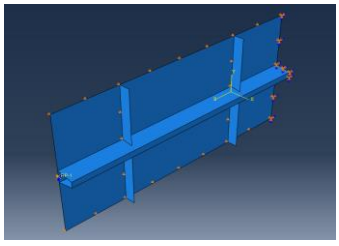

Fig. 3: Abaqus numerical model

Before that an evaluation of different models was performed. It was concluded that the best compromise between the simplified but accurate model is achieved by having two short panels to give the proper boundary conditions and some distance between the applied loads and the analysed central panel.

3.2 Material model

Following the von Mises criterion in the numerical calculation, the material model used behaves elastically until it reaches the yield stress f_y=690 MPa, with a Young's modulus equal to 210 GPa. Once the elastic properties of the material are fully utilized, a nominal hardening phase takes place until it reaches the ultimate resistance of the structure, f_u. The properties used to define the material model are listed in Table 1.

Table 1: Parameters used in the material model

E	E_{sh}	f_y	$f_{C1\varepsilon u}$	f_u	C_1
$210GPa$	$6{,}185GPa$	$690MPa$	$740MPa$	$770MPa$	0,61
ε_y	ε_{sh}	$C_1\varepsilon_u$	$C_2\varepsilon_u$	ε_u	C_2
0,33%	3%	3,81%	4,29%	6,23%	0,69

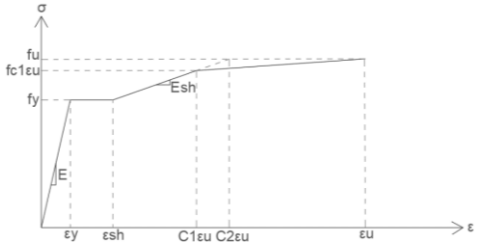

3.3 Equivalent geometric imperfections

In slender plate elements the geometric and material imperfections must be accounted for the structural strength´s calculation, once the collapse is governed by plate buckling. In addition, there is also the contribution of residual stresses, associated with the cutting and welding of the different plates. In that regard, it is essential to perform the modelling of the numerical models considering an equivalent geometric imperfection, as given in prEN 1993-1-5 [7]. Thus, 2 different types of equivalent geometric imperfections were developed, and a comparative analysis was carried out to determine which one should be used in the numerical models.

- **Equivalent geometric imperfection 1 (IMP 1) –** obtained by the combination of a stiffened panel global imperfection with a sine semi-wave shape and an amplitude of $h_w/400$, coupled with a local imperfection between sub-panels given by the shape of the first plate buckling mode with an amplitude of $b_i/200$ (Figure 4);
- **Equivalent geometric imperfection 2 (IMP 2) –** defined by the combination of a stiffened panel global imperfection of the with a sine semi-wave shape and an amplitude of $h_w/400$, coupled with a local imperfection between stiffeners also defined by a sine semi-wave shape with an amplitude of $b_i/200$ and considering the number of semi-waves equivalent to the first buckling mode, symmetrical to the longitudinal stiffener (Figure 4).

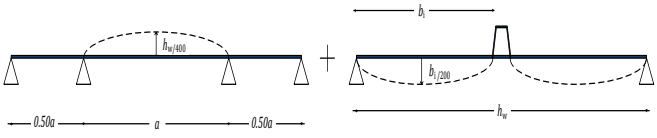

Fig. 4: Equivalent global and local imperfection

Modelling the initial imperfections using eigenmode shapes can be quite demanding, so in this investigation, for pure loads the first buckling modes were used (Figure 5 a), b) and c)) and in the case of a composition of loads, a combination of pure loads buckling modes was used, according to Figure 4 d), using amplitudes referred previously.

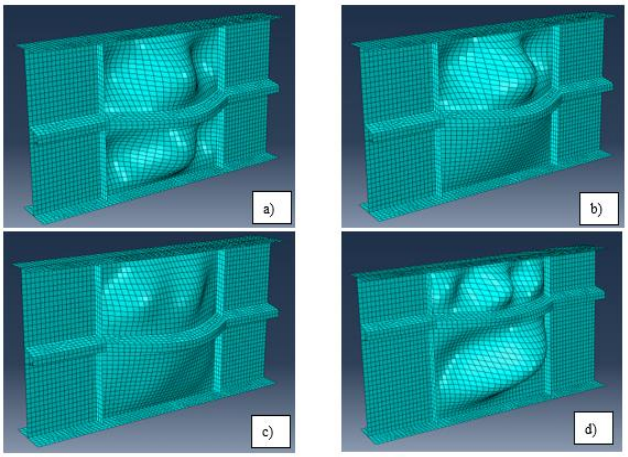

Fig. 5: Geometric imperfection based on first buckling mode due to a) compression; b) bending moment; c) shear; d) bending moment + shear

As geometrical imperfections are more important for N and M buckling modes, the ultimate resistance of a plate girder with six different stiffener positions subjected to compression and bending moment, simultaneously, was obtained using the numerical analysis software Abaqus [11]. The results obtained for the N-M interaction of the different geometries are presented in Figure 6, where the values are normalized to the ultimate resistances obtained for panels with IMP1 and one stiffener located at $0.50h_w$. From these results it can be concluded that the results match very well, although imperfection 2 is the one that generally gives the lowest resistances for each geometry. This is due to the fact that the number of semi-waves used is based on the shape of the buckling mode, which means that the buckling mode always needs to be assessed. Thus, IMP1 is selected as it gives the most reliable results.

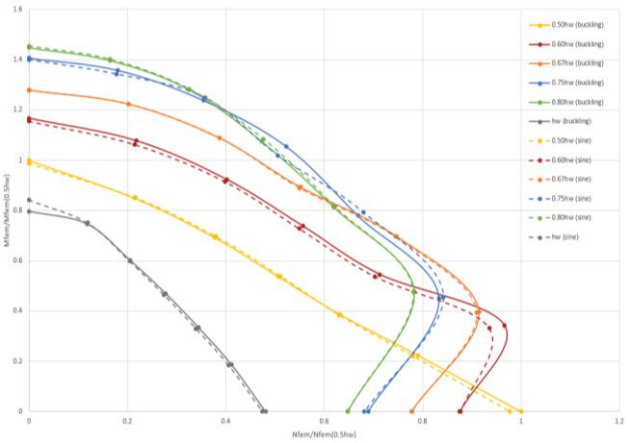

Fig. 6: Interaction N-M regarding the two cases of equivalent geometric imperfections and six different geometries

4. Numerical Results for N, M, V loadings

4.1 Analysis of the different numerical models

The analysis is based on the numerical models developed for each geometry of longitudinally stiffened slender plates, subjected to individually N, M, V loadings. Figure 7 presents the numerical models' resistances and the ones obtained by the prEN 1993-1-5 formulation for each loading. From this analysis, the following conclusions may be pointed out:

Conclusions on the $N_{b,FEM}/N_{b,Rk}$ analysis:

- Plate girders with longitudinal stiffeners in the compression part of the web have $N_{b,FEM}/N_{b,Rk} < 1.0$ meaning that, for these geometries, the numerically ultimate resistance is inferior to the one obtained by the standard. However, the dispersion of the obtained values is small if compared to the *M* and *V* loadings.

Conclusions on the $M_{eff,y,FEM}/M_{eff,y,Rk}$ analysis:

- Presents more conservative results but with greater dispersion. The numerical models provide resistances that are in general much higher than that obtained by the standard formulation. This is directly related to the possibility of almost total yielding of the tensioned sub-panel in the numerical calculation of $M_{eff,y,FEM}$, which is not considered when assessing $M_{eff,y,Rk}$ by the standard formulation.
- This is more noticeable if the stiffener is moved up, as it better protects the compressed panel that therefore practically do not buckle until it reaches yielding even on the compression side. The greater the redistribution (Figure 8), the greater the difference between the results given by the prEN 1993-1-5 [7] and the numerical models.

Conclusions on the $V_{bw,FEM}/V_{bw,Rk}$ analysis:

- The standard formulation gives always safe side results with a small deviation from the numerical model results.
- If the stiffener is moved up, the lower sub-panel becomes slenderer, decreasing the resistance to shear, confirmed by the prEN 1993-1-5 [7] and numerical model results.

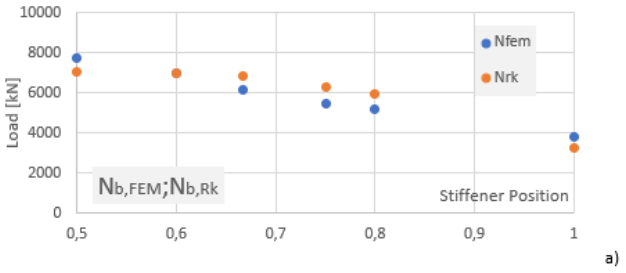

a)

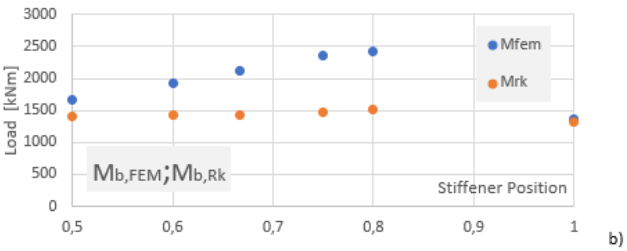

b)

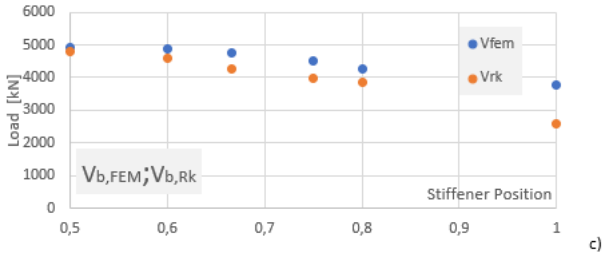

Fig. 7: Resistances of longitudinally stiffened web ($A_f/A_w = 0$): a) $N_{b,FEM}/N_{b,Rk}$; b) $M_{b,FEM}/M_{b,Rk}$; c) $V_{b,FEM}/V_{b,Rk}$

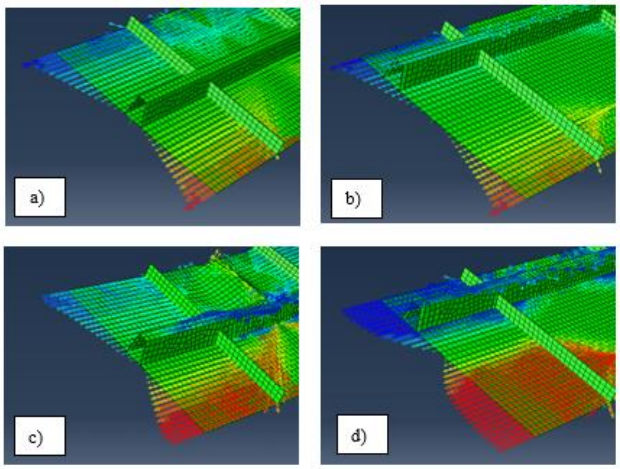

Fig. 8: Longitudinal stresses for the yielding bending moment and a) 0.50 h_w; b) 0.80 h_w and stress diagrams for maximum numerical resistances and c) 0.50 h_w; d) 0.80 h_w

4.2 Influence of the flanges on the calculation of the ultimate resistances

To understand the influence of the flanges in the ultimate resistance, plate girders with a ratio $A_f/A_w = 1.0$ were analysed. The ultimate resistances obtained are shown in Figure 9. The flanges make the model much more stable which, in turn, allows a huge gain in resistance for compression ($N_{f,Rd}$) and bending moment ($M_{f,Rk}$). In the presence of strong flanges, the prEN 1993-1-5 greatly overestimates the flange resistance to shear ($V_{f,Rk}$), as already referred by Jáger and Kövesdi [6]. These values are based on the calculation of the distance between the plastic hinges, c. André Reis and Biscaya [8] proposed different c values that lead to better estimates of the shear resistances in relation to the numerical model results.

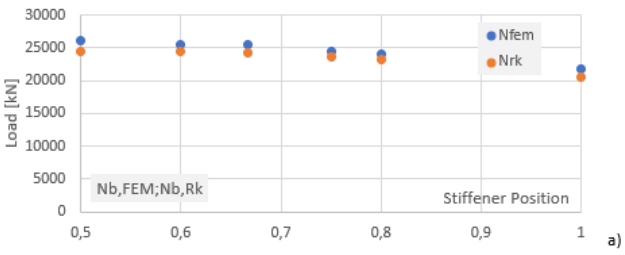

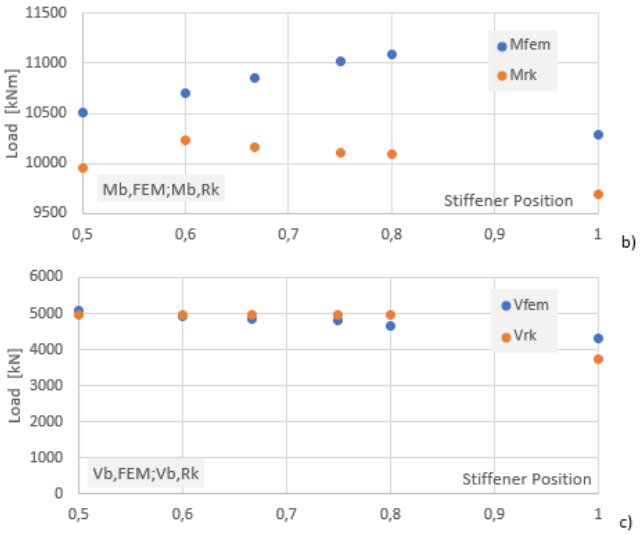

Fig. 9: Resistances of a plate girder with $A_f/A_w = 1.0$: a) $N_{b,FEM}/N_{b,Rk}$; b) $M_{b,FEM}/M_{b,Rk}$; c) $V_{b,FEM}/V_{b,Rk}$

5. Study of the N-M-V interaction

5.1 N-M and M-V interaction

Figure 10 presents the N-M and M-V interactions for different plate girder geometries with and without flanges. It can be concluded that using the middle stiffener is the compromise, working well for positive and negative moments and for cases of N and V acting separately, it is always the best option. For N-M-V loadings, the stiffener position must be optimized depending on the governing load. For the situation without flanges, it would be interesting to move the stiffener up as there is a very high increase of bending resistance. As the bending moment introduces compression on the top sub-panel, the stiffener higher up increases the working resisting area and avoids local buckling of the web sub-panel. However, the stiffener position becomes much less relevant for plate girders with strong flanges, as for $A_f/A_w = 1.0$.

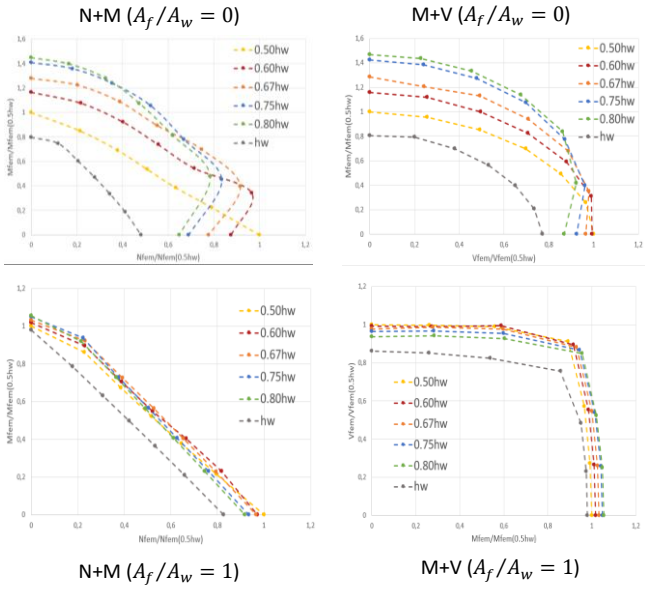

Fig. 10: N-M and M-V interaction for stiffened plate girders with different positions of the stiffener

5.2 N-M-V interaction following the new proposal

Results of the N-M-V interaction resistance for diferent rations between loads were determined using the new proposal [9] and the numerical models (Fig. 11). The relative results obtained with the numerical models are presented in Figure 12, which show the behaviour observed for two ratios of A_f/A_w (= 0 – without flanges, and = 1 – with strong flanges). Without flanges the dispersion of the results is much higher, and the new proposal results are in general conservative, although for some geometries they can give unsafe results.

When adding the flanges, the plate girder behaviour becomes more stable and consequently has a much smaller dispersion between the resistances obtained by the numerical analysis and the new proposal. As the stiffener shifts up, the values tend to become more dispersed in both cases, due to the fact that the individual resistances to V and M become more conservative.

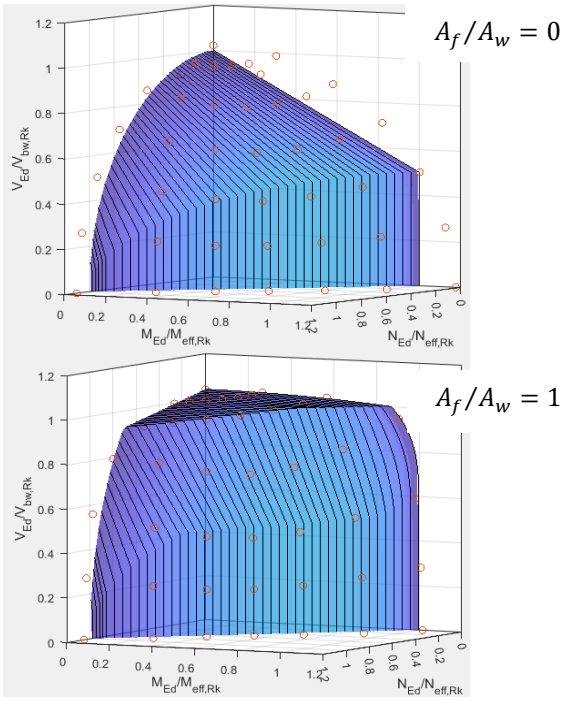

Fig. 11: R_{FEM}/R_{PROP} for plate girders with a longitudinal stiffener at 0.50 h_w and $A_f/A_w = 0$ or 1.0

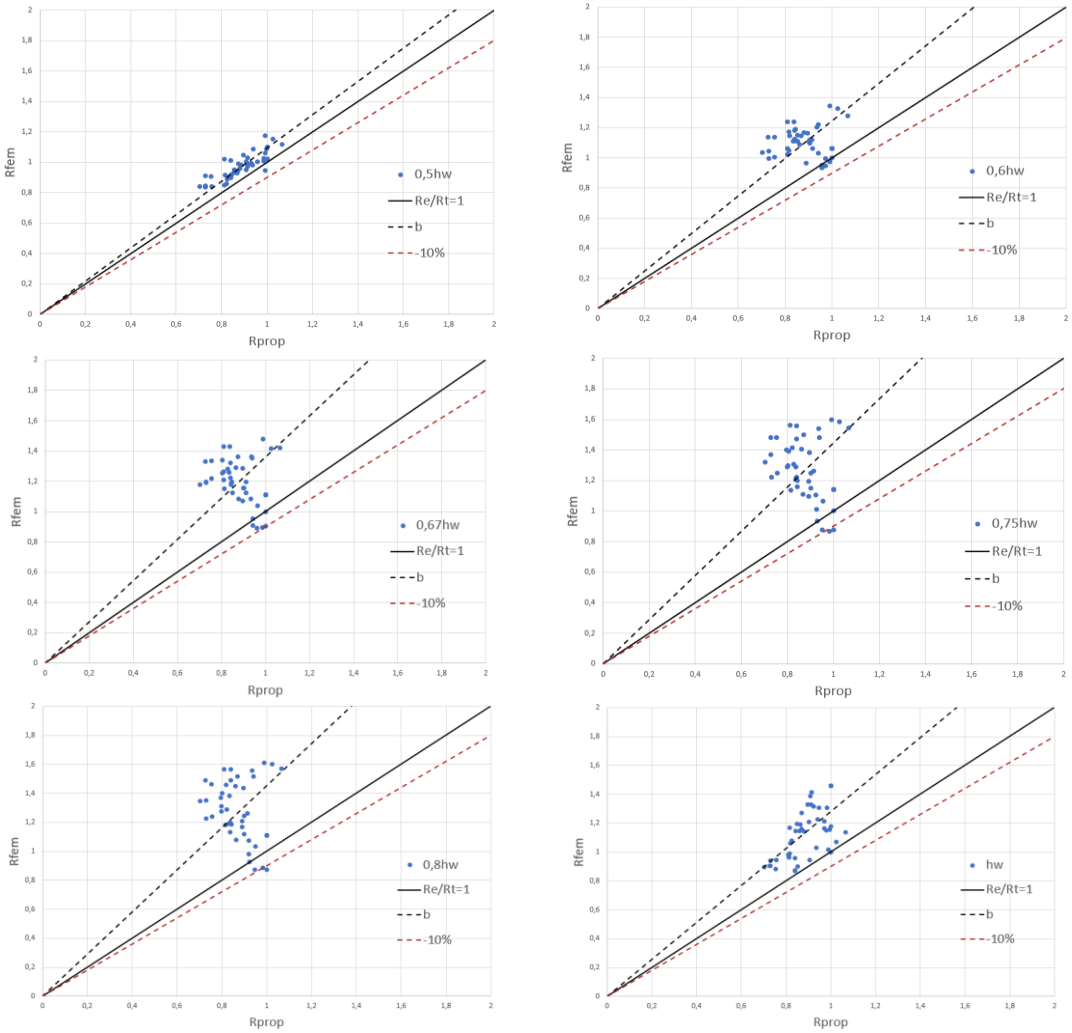

R_{FEM}/R_{PROD} $(A_f/A_w = 0)$

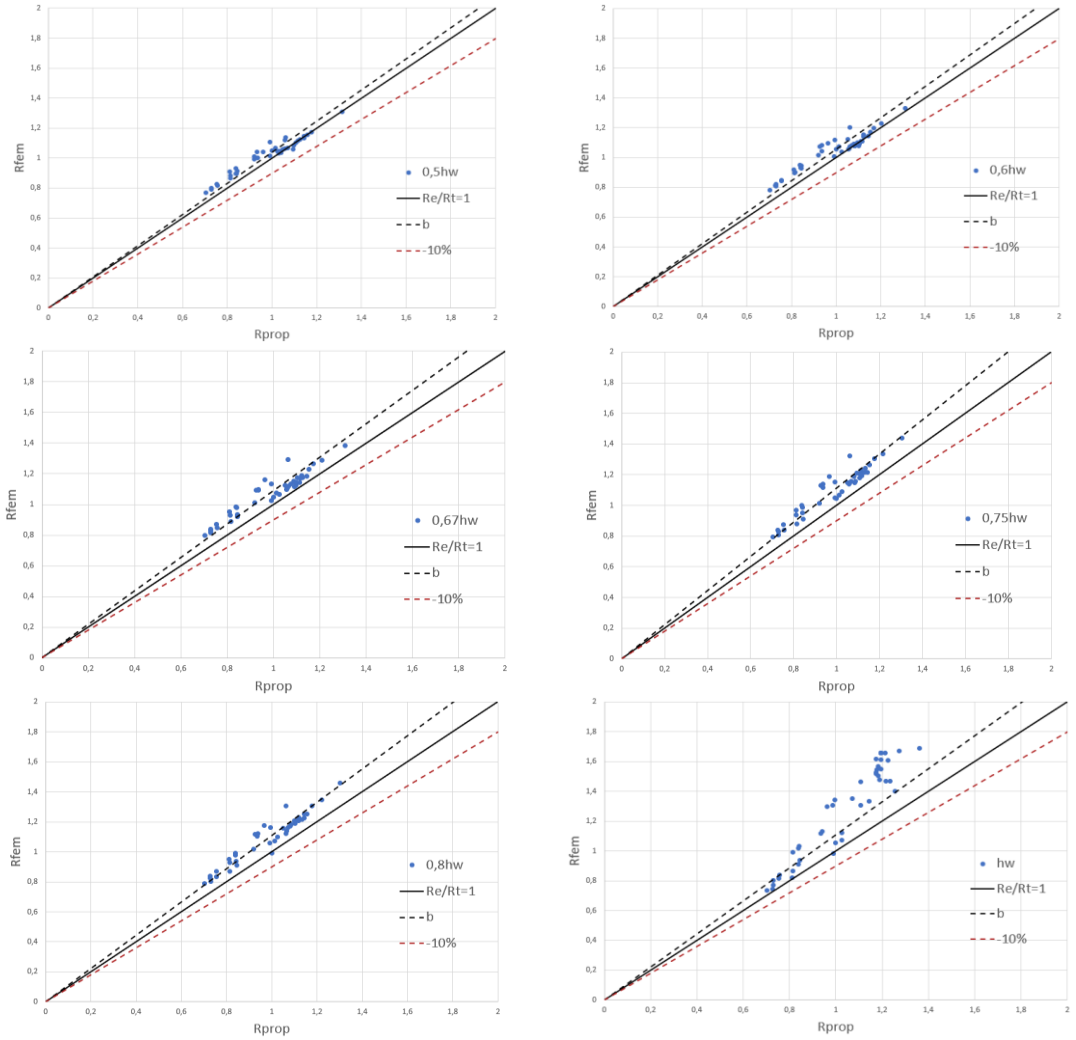

R_{FEM}/R_{PROP} $(A_f/A_w = 1.0)$

Fig. 12: R_{FEM}/R_{PROP} for plate girders with six longitudinal stiffener positions and $A_f/A_w = 0$ or 1.0

6.Post maximum load behaviour

It is also of interest to evaluate the behaviour of the plate girder after reaching its maximum capacity, depending on the type of loading and failure mode, as well as, on the plate girder slenderness and its capacity to redistribute the stresses after reaching the maximum load capacity.

To evaluate the post maximum load capacity of the plate girder, the arc-length parameter is assumed to be a good parameter to evaluate the behaviour during the process of loading. For the N, M and V loadings, applied separately in the plate girder, Figure 13 presents the LPF and arc-length plots, considering the stiffened web without flanges $\frac{A_f}{A_w} = 0$ (dash lines) and with strong flanges $\frac{A_f}{A_w} = 1$ (solid lines).

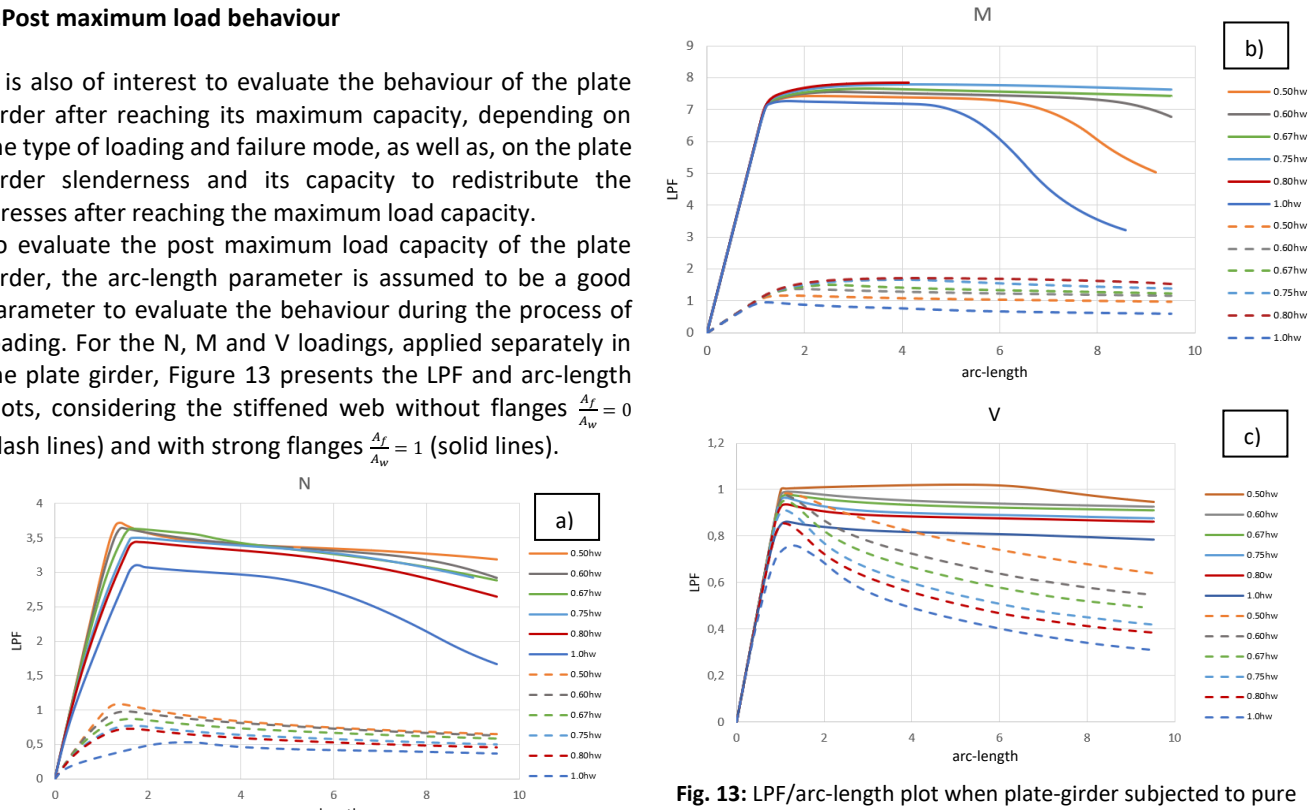

Fig. 13: LPF/arc-length plot when plate-girder subjected to pure a) compression, b) bending moment and c) shear

If the plate-girder is subjected to the axial load, the maximum resistance is much lower than when strong flanges are adopted. The increase of resistance when the flanges are added is even higher than the factor of 3 of the increased area, due to the fact that the flanges do not buckle at the same time of the web. In all cases a local plate buckling mode was reported which explains why after reaching the maximum plate girder capacity, very high loads can still be equilibrated with increasing deformations. This behaviour is more noticeable if the longitudinal stiffener is placed at mid-height of the web, dividing the web in two sub-panels with the same buckling behaviour whereas the worst-case scenario is if no stiffener is used.

For the case of a bending moment, when the flange is added, the load capacity of the plate girder is much reduced after reaching the maximum resistance because the buckling mode also involves the buckling of the compressed flange into the web, known as flange induced buckling. However, if the longitudinal stiffener is near the top compressed flange, like at $0.80h_w$, the web is prevented to buckle, and the bending capacity is preserved. If no flanges are used, the resistant capacity is kept almost constant after reaching the maximum, since no buckling occurs in the top sub-plate until reaching the complete yielding of the cross-section.

Finally, for the case of plate girders subjected to shear forces a local typical shear plate buckling mode was reported. The gains of using a longitudinal stiffener are significant, dividing the web into two sub-panels, but the difference of adding flanges is not so pronounced. Since the longitudinal stiffener is very stiff, it perfectly divides the web into two sub-panels, sometimes even with two buckling semi-waves. The highest shear resistance is obtained if the stiffener is placed at mid-height of the web and is reduced if the stiffener is moved up or suppressed. Without flanges, the stiffened plate loses significant shear capacity after reaching the maximum load being more visible for slender sub-panels (stiffener moved up). By adding the flanges, although there is not a huge gain in the maximum plate girder shear capacity, it remains practically unchanged with increase deformations, due to the fact that the edges of the buckle web remained supported by the flanges.

7.Application of the Reduced Stress Method with Shedding

7.1 Results for the N, M and V loadings

The analysis is based on the comparison of both calculation methods (RSM and EWM), when plate-girders are subjected to individually N, M, V loadings, shown in Figure 14.

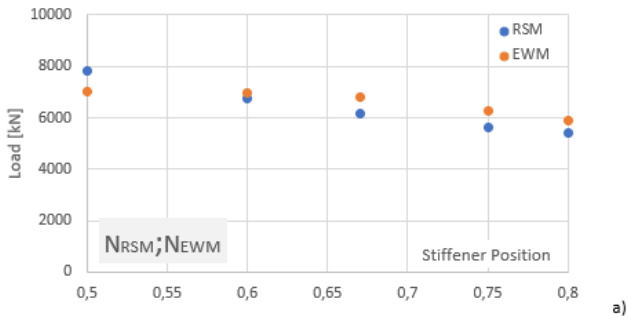

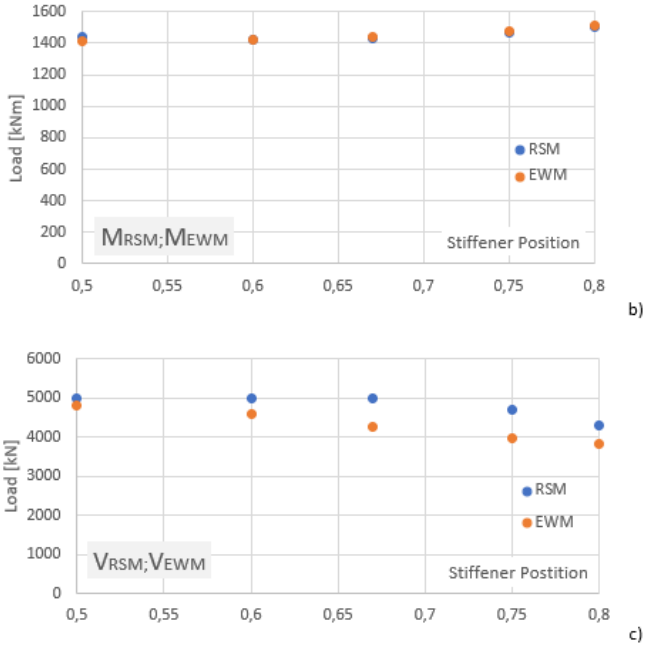

Fig. 14: Stiffened plate resistances (with $A_f/A_w = 0$): a) N_{RSM}/N_{EWM}; b) M_{RSM}/M_{EWM}; c) V_{RSM}/V_{EWM}

Conclusions on the $\mathbf{N_{RSM}/N_{EWM}}$ analysis:

- In the EWM the effective widths assume a certain redistribution and for relatively narrow sub-plates this redistribution is small. However, the larger the sub-panel (the higher the stiffener is), the greater the redistribution, thus moving apart from the elastic behaviour as it is assumed in the RSM.
- For the RSM points, there is a linear variation when shifting the stiffener up caused by the reduction of the local critical stress due to the fact that the slenderest panel will govern the resistance.

Conclusions on the $\mathbf{M_{RSM}/M_{EWM}}$ analysis:

- The resistances are the same irrespective of the method used. This happens because there is no web buckling hence there is no redistribution of stresses (elastic distribution is maintained) corresponding to the yielding bending moment for both methods.

Conclusions on the $\mathbf{V_{RSM}/V_{EWM}}$ analysis:

- The shear resistance given by the RSM is always higher than that of the EWM because values of critical stresses determined by EBP are used, higher than that of the prEN 1993-1-5- Annex A formulation which is more conservative.

7.2 Influence of the flanges on the calculation of the ultimate resistance

To understand the influence of the flanges on the resistances determined by the RSM, plate girders with a ratio $A_f/A_w = 1.0$ were analysed. The ultimate resistances obtained are shown in Figure 15. The RSM neglects the contribution of the flanges to the resistance, therefore, as it was expected, the values obtained by the EWM are always higher when adding flanges to the model. For the case of the plate girder only subjected by shear, there are no differences on the values obtained by the RSM whether in the presence of flanges or not, because the resisting area, A_w, is kept constant.

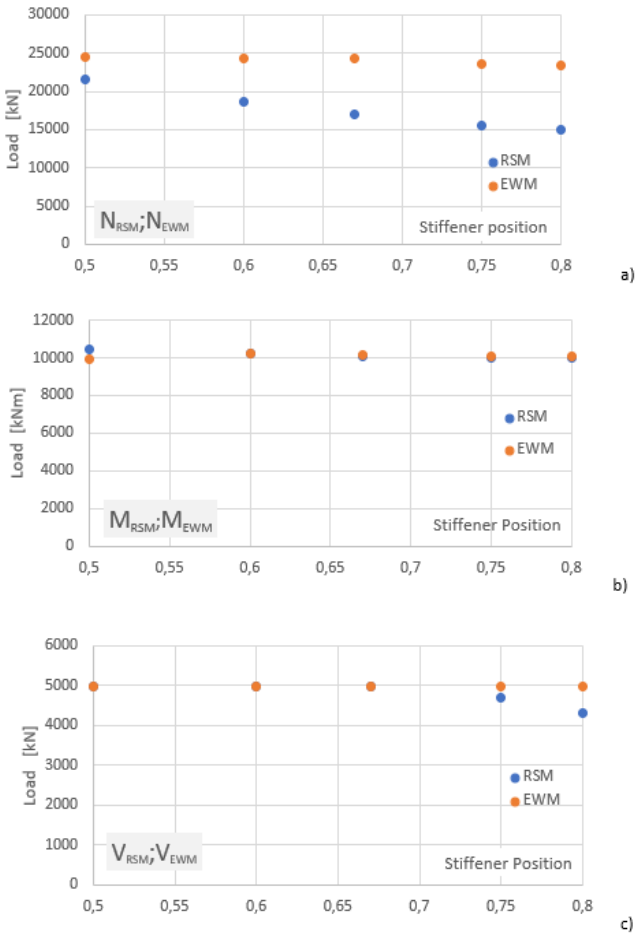

Fig. 15: Plate girder resistances (with $A_f/A_w = 1.0$): a) N_{RSM}/N_{EWM}; b) M_{RSM}/M_{EWM}; c) V_{RSM}/V_{EWM}

7.3 Study of the N-M-V interaction

Results of the N-M-V interaction surface from RSM and FEM points are shown in Figure 16 as well as the resistance for different load cases determined using both proposals according to the prEN 1993-1-5 (RSM and EWM) and the numerical models previously discussed are presented in Figure 17, which show the behaviour observed for two ratios of A_f/A_w (= 0 – without flanges, and = 1 – with strong flanges).

Conclusions on the N-M-V analysis:

$A_f/A_w = 0$

- Although the differences are not higher than 10%, the RSM is being estimated with a resistance greater than what we get in most ABAQUS models since the normalized slenderness, $\bar{\lambda}_p$(maximum between the local slenderness of the sub-panel and the global), and the shape of the N-V interaction graphic are not the same.
- The RSM has a quadratic shape because the bases come from a von Mises formula while the N-V interaction does not, especially when it comes to slenderer plates, which is the case, there is a bigger difference between the two thus giving results that are not always on the safety side.
- It can be seen in Figure 16 that in the N-V plane the RSM is overestimated compared to the numerical models, while the actual behaviour is approximately an ellipse for the two methods along the plane M-V.
- The RSM is supposed to have higher resistances than the EWM for the cases without flanges, because it applies the concept of a global slenderness of the web as well as a reduction factor based on the von Mises formula, which is closer to reality.

$A_f/A_w = 1.0$

- When adding strong flanges, much better values of the average and dispersion are obtained.
- Because the prEN 1993-1-5 neglects the flanges contribution to the resistance, this design gives conservative resistances.

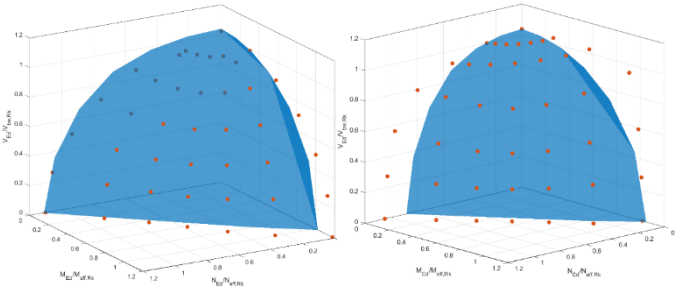

$A_f/A_w = 0$ $A_f/A_w = 1$

Fig. 16: N-M-V interaction surface from RSM and FEM points

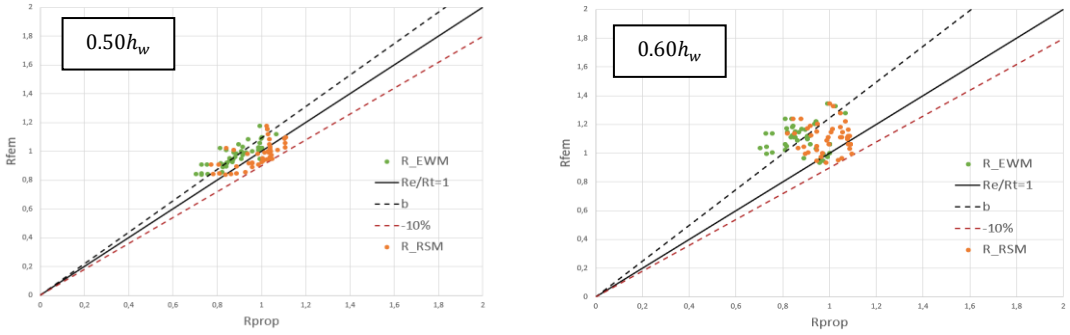

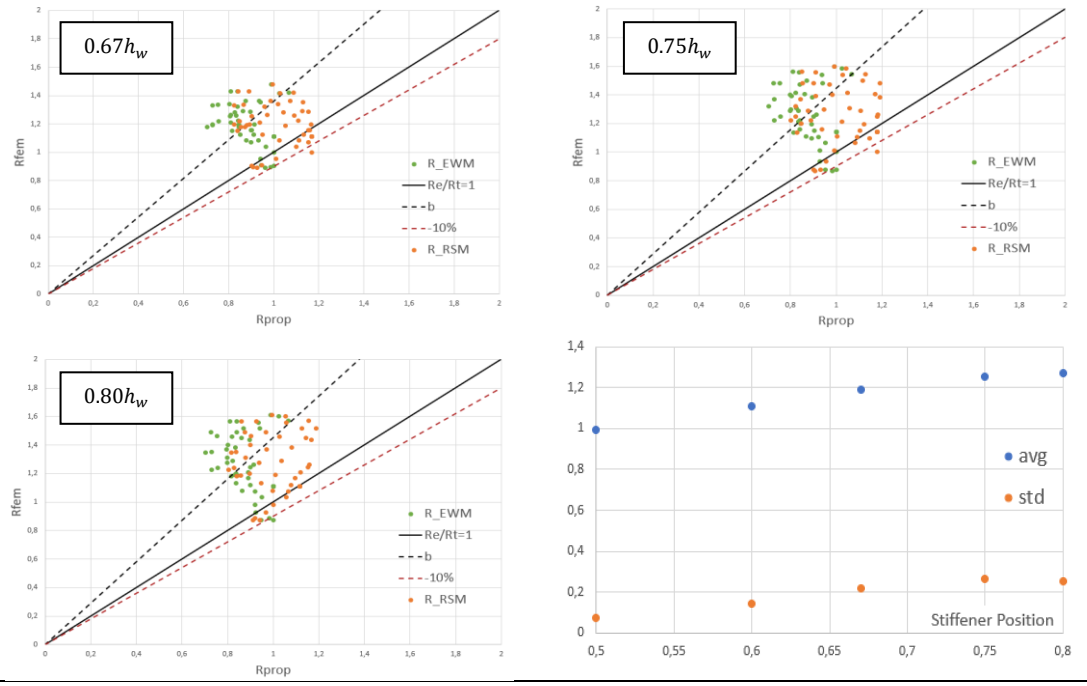

R_{RSM}/R_{EWM} $(A_f/A_w = 0)$

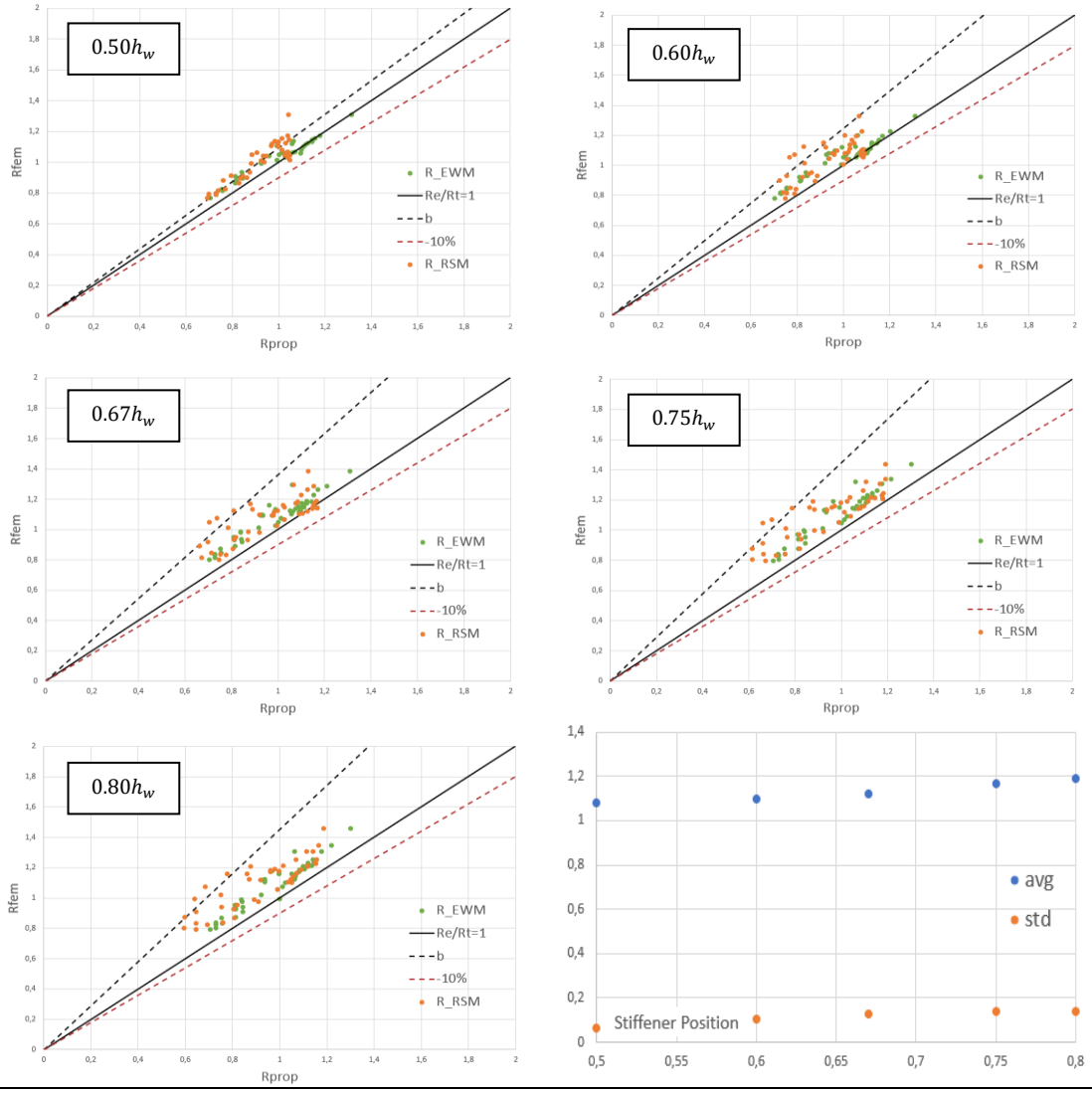

R_{FEM}/R_{PROP} $(A_f/A_w = 1.0)$

Fig. 17: R_{RSM}/R_{FEM} for plate girders with five longitudinal stiffener positions and $\frac{A_f}{A_w} = 0$ or 1.0

7.4 RSM+S for N and M loads

After evaluating the ultimate resistance of the plate girders when subjected to compression, bending moment and shear using the RSM as it is proposed in the prEN 1993.1.5, it is intended to use the RSM+S to assess what results can be improved when compared to the numerical resistances.

For these plate-girders, if the bending moment is applied, the resistance is equal to the yielding bending moment, so no shedding is possible from the web to the flanges and thus no improvement can be archived for this case. For pure compression, the ultimate resistances obtained with the possibility of shedding tend to be much more similar to the ones obtained by the numerical models, as well as those of the EWM (Figure 18).

Therefore, the RSM with stress shedding gives much better results than when neglecting the flanges contribution. As the stiffener is shifted up, the coefficient k tends to become smaller (Figure 19), indicating that there is a greater possibility of redistribution even if most of the normal stresses remain in the web (between 0.65 and 0.85).

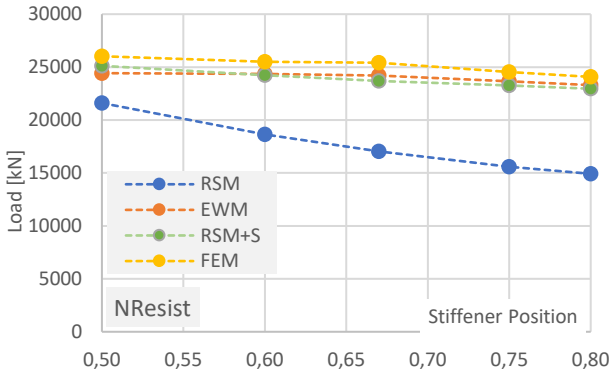

Fig. 18: Comparison of the pure compression resistance to between the 3 methods and the FEM results

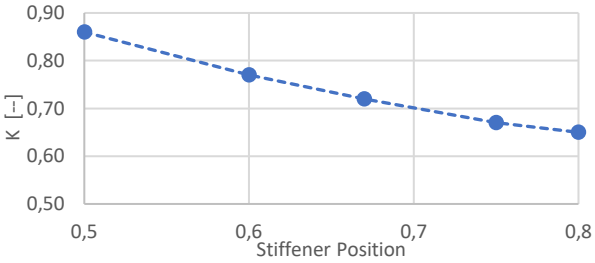

Fig. 19: Values of k for the different stiffener positions

7.5 RSM+S for N-M interaction

Finally, the influence of shedding on the N-M interaction is analysed for plate girder with stiffener at mid height of the section ($0.50h_w$) and flanges with $A_f/A_w = 1.0$.

Figure 20 presents the comparison between the N-M interaction for the different load cases (with $\theta_1 = [0, 15, 30, 45\ 60{,}75, 90]$ and $\theta_2 = 0$).

The RSM+S presents the N-M interaction surface closest to those obtained through the numerical models (FEM). Both the EWM and RSM+S produce an approximate linear form when the stiffener is located at mid-height, however, the N and M resistances obtained by the EWM are a little more conservative.

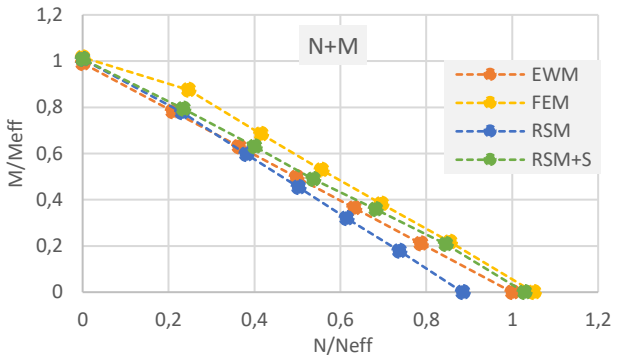

Fig. 20: Interaction N-M for the three methods and the FEM results

8. Conclusions and some further research works

From the studies on the N-M-V interaction of high strength steel S690 plate girders with one longitudinal stiffener, the following conclusions can be drawn:

- Three panel FE models should be adopted with the loads applied at the edge of the lateral panels, to minimize the effect on the middle panel that is being analysed.
- The shape of the equivalent imperfection based on the first buckling N, M, V modes works well but it was necessary to combine these modes to analyse N-M-V interaction loadings.
- The new N-M-V interaction formulas [8] prove to be well calibrated for high strength steel S690 plate girders with various positions of the longitudinal stiffener.
- For N and V loadings the longitudinal stiffener should be placed at the middle of the panel; for high M a greater resistance is achieved by moving up the stiffener to the compressive part of the web. For the N-M-V loading, the best position of the longitudinal stiffener depends on the governing internal force.
- When no shedding is assumed, the RSM gives, in general, higher resistances to N, M and V separately compared to EWM because the critical stresses obtained using the EBP are higher than the ones obtained by the approximate formulations. Adding the flanges, the results reverse since the RSM neglects the contribution of the flanges. Regarding the N-M-V interaction study, as the RSM has a quadratic shape, it ends up providing results against safety, namely for slender plate girders.
- Finally, the RSM with stress shedding as proposed by Biscaya proposal provides very consistent results, being the closest ones to the ultimate resistances obtained by the numerical models.

Several aspects deserve further research, namely:

- Obtaining an N-M-V interaction formulation that can be applicable to cases where one longitudinal stiffener is located in the tensioned or compressed diagonal.
- Development of an expression or a figure that can provide the value of k as function of the web slenderness and ratio between the area of the flanges and the web.
- Extend the application of the RSM+S method to plate girders with other geometries and submitted to combined loads of bending moment with normal and shear forces.

References

[1] EN 1993-1-5 – *Eurocode 3 – Design of steel structures – Part 1-5: Plated structural elements*, CEN, 2005.

[2] F. Sinur – *Behaviour of longitudinally stiffened plate girders subjected to bending-shear interaction*, University of Ljubljana, PhD Thesis, 2011.

[3] F. Sinur; D. Beg – *Moment-shear interaction of stiffened plate girders – Numerical study and reliability analysis*, J. Constr. Steel Res. 88, pags. 231-243, 2013.

[4] B. Jáger; B. Kövesdi; L. Dunai – *I-girders with unstiffened slender webs subjected by bending and shear interaction*, J. Constr. Steel Res. 131, 2017.

[5] B. Jáger; B. Kövesdi; L. Dunai – *Numerical investigations on bending and shear buckling interaction of I-Girders with slender web*, Thin-Walled Structures, 143, 2018.

[6] B. Jáger; B. Kövesdi; L. Dunai – *Bending and shear buckling interaction behaviour of I-girders with longitudinally stiffened webs*, J. Constr. Steel Res. 145, 2018.

[7] prEN 1993-1-5 – *Eurocode 3 – Design of steel structures – Part 1-5: Plated structural elements*, CEN, 2021.

[8] A. Biscaya – *Buckling resistance of steel plated girders considering M-V interaction with high compression forces*, PhD Thesis, Instituto Superior Técnico, 2021.

[9] A. Biscaya, H. Afonso, J. O. Pedro – *New proposal for the N-M-V design interaction of steel plate girders – Application to S690 high-strength steel*, Congresso CMM, 2021.

[10] H. Afonso – *Dimensionamento de Vigas de Secção Soldada com Aço S690 Sujeitas a Esforços Combinados de Flexão, Corte e Compressão*, MSc Dissertation, IST, 2021.

[11] SIMULIA, *Abaqus Scripting User´s Manual. Dassault Systems*, 2011.